

## Research Article

# 2D DOA Estimation with a Two-Parallel Array Consisting of Two Uniform Large-Spacing Linear Arrays

Sheng Liu,<sup>1</sup> Jing Zhao,<sup>1</sup> and Yu Zhang<sup>1b2</sup>

<sup>1</sup>School of Data Science, Tongren University, Tongren 554300, China

<sup>2</sup>College of Computer and Information Science, Southwest University, Chongqing 400715, China

Correspondence should be addressed to Yu Zhang; zhangyuswu@163.com

Received 16 February 2020; Revised 1 April 2020; Accepted 9 April 2020; Published 30 April 2020

Academic Editor: Giorgio Montisci

Copyright © 2020 Sheng Liu et al. This is an open access article distributed under the Creative Commons Attribution License, which permits unrestricted use, distribution, and reproduction in any medium, provided the original work is properly cited.

In this paper, an improved propagator method (PM) is proposed by using a two-parallel array consisting of two uniform large-spacing linear arrays. Because of the increase of element spacing, the mutual coupling between two sensors can be reduced. Firstly, two matrices containing elevation angle information are obtained by PM. Then, by performing EVD of the product of the two matrices, the elevation angles of incident signals can be estimated without direction ambiguity. At last, the matrix product is used again to obtain the estimations of azimuth angles. Compared with the existed PM algorithms based on conventional uniform two-parallel linear array, the proposed PM algorithm based on the large-spacing linear arrays has higher estimation precision. Many simulation experiments are presented to verify the effect of proposed scheme in reducing the mutual coupling and improving estimation precision.

## 1. Introduction

Estimating the directions of arrival (DOA) of spatial signals by sensors array has widespread application in wireless communication [1] and multiple input multiple output (MIMO) radar [2]. Two-dimensional (2D) DOA estimation technology can obtain more angle information of spatial signals, and it has higher practical significance than one-dimensional (1D) DOA estimation technology. L-shaped array and parallel array are frequently used array constructions for 2D DOA estimation. The L-shaped array consists of two orthogonal linear arrays, based on which many effective 2D DOA estimation algorithms [3, 4] were proposed.

Being different from the L-shaped array, the parallel array consists of multiple parallel linear arrays and has more diverse array geometries. Many 2D DOA estimation algorithms [5–10] were designed based on parallel arrays. In [5], a DOA matrix algorithm was proposed to obtain the estimations of the elevation and azimuth angles by using a two-parallel linear array. In [6], the polynomial rooting technology was used for 2D DOA estimation based on a two-

parallel linear array. In [7], a rank-reduction algorithm based on a three-parallel linear array has presented for 2D DOA estimation. However, the three algorithms need to perform eigenvalue decomposition (EVD) or singular value decomposition (SVD) of covariance matrix. The propagator method (PM) [8–13] gains extensive attention for the lower computational complexity because it does not need to perform EVD of covariance matrix. In [8], authors used PM algorithm to estimate 2D DOA by multiple parallel linear arrays. In [9], a modified 2D PM algorithm based on two-parallel linear array was proposed for improving estimation precision. In [10], another modified 2D PM algorithm based on three-parallel linear array was proposed for reducing computational complexity. In [11], PM algorithm was used with the parallel factor analysis (PARAFAC) model to estimate the 2D DOA, where the PARAFAC model is solved by circulative iteration.

But we should notice that all the algorithms [5–11] are based on uniform array, the interval of adjacent sensors cannot exceed half-wavelength of the incident signal. In fact, mutual coupling inevitably exists between two sensors, particularly for the closed two sensors. Aiming to extend

array aperture and reduce mutual coupling, some nonuniform sparse array constructions such as nested array [14–17] and coprime array [18–20] were proposed. Nested array consists of multiple subarrays with different intervals. Coprime array consists of two uniform linear arrays, and the intervals of two subarrays are relevant to two mutual prime integers. Compared with the uniform array, nonuniform sparse arrays have extendable array aperture and higher degree of freedom. For the sparse arrays [14–19], the interval of adjacent sensors can exceed half a wavelength of the incident signal which can reduce the mutual coupling. Despite all these, in order to avoid direction ambiguity, the minimum element spacing of these sparse arrays still cannot exceed half-wavelength of the incident signal. Hence, it is difficult to eliminate mutual coupling completely. In [20], authors proposed an off-grid DOA estimation algorithm based on an unfolded parallel coprime array. The mutual coupling of array can be reduced to a great extent. In addition, for non-uniform sparse arrays, constructing extended covariance matrix is a universal method to exploit the potential virtual sensors. But the computational complexity of the DOA estimation algorithms is closely related to the order of covariance matrix. This method can improve performance of angle estimation, but also can increase computational complexity.

In this paper, we propose a two-parallel linear array consisting of two uniform large-spacing linear arrays. The element spacing is  $q$  units for one linear array and  $q + 1$  units for the other linear array, where  $q$  is not smaller than 2. Hence, the mutual coupling in one linear array can be eliminated when  $q$  is selected properly. For avoiding direction ambiguity, an improved 2D PM algorithm also is proposed to estimate the elevation and azimuth angles. Compared with the PM [8–10], the proposed algorithm has two obvious advantages: (1) the proposed algorithm can reduce the mutual coupling considerably due to the use of large-spacing linear array; (2) the proposed algorithm has higher estimation precision than PM [8–10], even if the mutual coupling between sensors is ignored.

## 2. Array Received Model

Consider that two uniform large-spacing parallel arrays are located on the  $xoz$  plane, as shown in Figure 1. The coordinates of the  $N + 1$  sensors on  $z$  axis are  $\{0, 0, 0\}, \{0, 0, qd\}, \dots, \{0, 0, qNd\}$ , where  $d = (\lambda/2)$ ,  $\lambda$  is the wavelength of incident signal, and  $q(q < N)$  is any integer no less than 2. The coordinates of the  $N$  sensors for the other subarray are  $\{d, 0, 0\}, \{d, 0, (q+1)d\}, \dots, \{d, 0, (q+1)(N-2)d\}, \{d, 0, (q+1)(N-1)d\}$ . Figure 2 shows the construction of a 17-element large-spacing two-parallel linear array with  $q=2$ , and Figure 3 shows the construction of a traditional 17-element two-parallel linear array [8, 9].

If we assume that mutual coupling exists between two sensors with the interval no further than  $d$ , we can see that mutual coupling only exists in three pairs of sensors from Figure 2. Obviously, from Figure 3, we can find that the coupling effect exists between any adjacent sensors for the conventional two-parallel linear array.

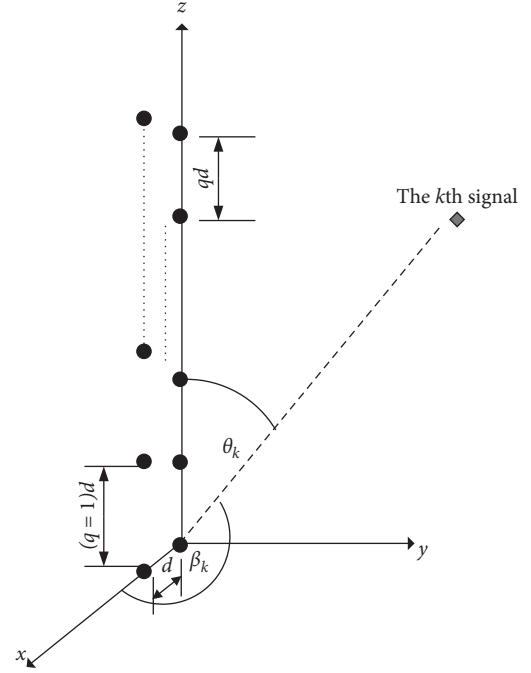


FIGURE 1: Construction of proposed two-parallel linear array.

Suppose that  $K(K < N)$  far-field, uncorrelated, narrowband signals received by the proposed array. We define the elevation angle and azimuth angle of the  $k$ th signal as  $\theta_k$  and  $\beta_k$ , respectively. Let received vectors by the two large-spacing linear arrays be  $\mathbf{z}(t) = [z_1(t), z_2(t), \dots, z_{N+1}(t)]^T \in C^{(N+1) \times 1}$ , and  $\mathbf{x}(t) = [x_1(t), x_2(t), \dots, x_N(t)]^T \in C^{N \times 1}$ , respectively. If we ignore the effect of mutual coupling,  $\mathbf{z}(t)$  and  $\mathbf{x}(t)$  can be written as [6, 10]

$$\begin{cases} \mathbf{z}(t) = \mathbf{A}(\boldsymbol{\theta})\mathbf{s}(t) + \mathbf{n}_z(t), \\ \mathbf{x}(t) = \mathbf{B}(\boldsymbol{\theta})\boldsymbol{\Phi}(\boldsymbol{\beta})\mathbf{s}(t) + \mathbf{n}_x(t), \end{cases} \quad t = 1, 2, \dots, T, \quad (1)$$

where  $\boldsymbol{\theta} = [\theta_1, \dots, \theta_K]$ ,  $\boldsymbol{\beta} = [\beta_1, \dots, \beta_K]$ ,  $\mathbf{A}(\boldsymbol{\theta}) = [\mathbf{a}(\theta_1), \dots, \mathbf{a}(\theta_K)] \in C^{(N+1) \times K}$ ,  $\mathbf{a}(\theta_k) = [1, e^{-j2\pi qd \cos \theta_k / \lambda}, \dots, e^{-j2\pi q(N-1)d \cos \theta_k / \lambda}]^T \in C^{(N+1) \times 1}$ ,  $\mathbf{B}(\boldsymbol{\theta}) = [\mathbf{b}(\theta_1), \dots, \mathbf{b}(\theta_K)] \in C^{N \times K}$ ,  $\mathbf{b}(\theta_k) = [1, e^{-j2\pi(q+1)d \cos \theta_k / \lambda}, \dots, e^{-j2\pi(q+1)(N-2)d \cos \theta_k / \lambda}, e^{-j2\pi(q+1)(N-1)d \cos \theta_k / \lambda}]^T \in C^{N \times 1}$ ,  $\boldsymbol{\Phi} = \text{diag}\{e^{-j2\pi d \cos \beta_1 / \lambda}, e^{-j2\pi d \cos \beta_2 / \lambda}, \dots, e^{-j2\pi d \cos \beta_K / \lambda}\}$ ,  $\mathbf{n}_z(t) = [n_{z,1}(t), n_{z,2}(t), \dots, n_{z,N+1}(t)]^T \in C^{(N+1) \times 1}$ , and  $\mathbf{n}_x(t) = [n_{x,1}(t), n_{x,2}(t), \dots, n_{x,N}(t)]^T \in C^{N \times 1}$  are white Gaussian noise vectors received by the two linear arrays.

Let  $\mathbf{y}(t) = \begin{bmatrix} \mathbf{z}(t) \\ \mathbf{x}(t) \end{bmatrix}$ , then we have

$$\mathbf{y}(t) = \begin{bmatrix} \mathbf{A}(\boldsymbol{\theta}) \\ \mathbf{B}(\boldsymbol{\theta})\boldsymbol{\Phi}(\boldsymbol{\beta}) \end{bmatrix} \mathbf{s}(t) + \begin{bmatrix} \mathbf{n}_z(t) \\ \mathbf{n}_x(t) \end{bmatrix}. \quad (2)$$

If we assume that mutual coupling exists in array,  $\mathbf{y}(t)$  can be expressed as [19, 20]

$$\mathbf{y}(t) = \mathbf{M} \begin{bmatrix} \mathbf{A}(\boldsymbol{\theta}) \\ \mathbf{B}(\boldsymbol{\theta})\boldsymbol{\Phi}(\boldsymbol{\beta}) \end{bmatrix} \mathbf{s}(t) + \begin{bmatrix} \mathbf{n}_z(t) \\ \mathbf{n}_x(t) \end{bmatrix}, \quad (3)$$

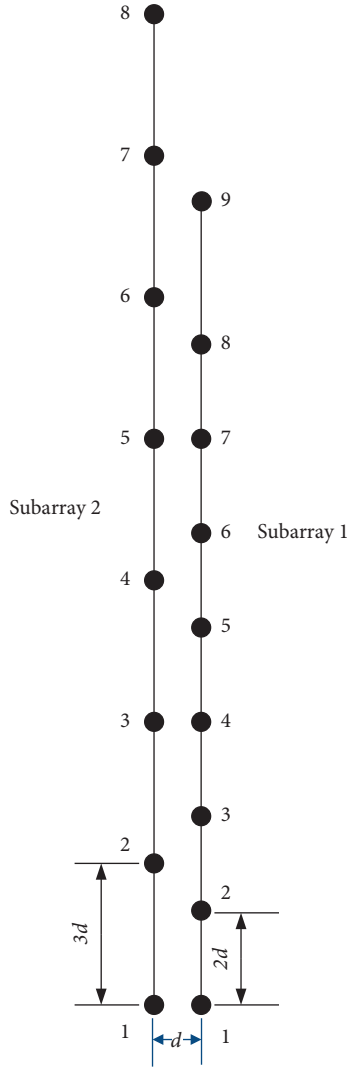
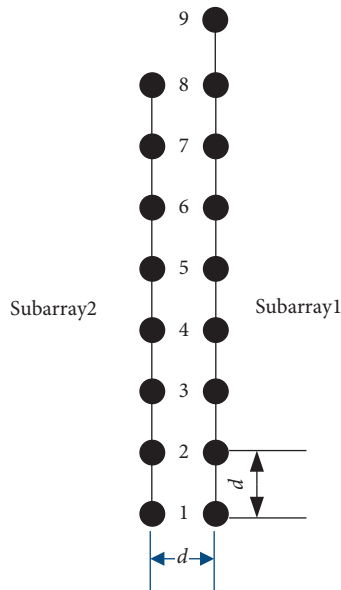
FIGURE 2: Two uniform large-spacing parallel linear arrays ( $q=2$ ).

FIGURE 3: Two uniform parallel linear arrays [8, 9].

where  $\mathbf{M} = (m_{ij})_{(2N+1) \times (2N+1)}$  is the mutual coupling matrix and  $m_{ij}$  is the mutual coupling coefficient between the  $i$ th sensor and the  $j$ th sensor. Here, we let the  $i$ th sensor be the  $i$ th sensor of the first array for  $i \leq N+1$  and be the  $(i-N-1)$ th sensor of the second array for  $i > N+1$ .

The total mutual coupling of an array can be reflected in coupling leakage [17] as

$$\text{CL}(\mathbf{M}) = \frac{\|\mathbf{M} - \tilde{\mathbf{M}}\|_F}{\|\mathbf{M}\|_F}, \quad (4)$$

where  $\tilde{\mathbf{M}} = (\tilde{m}_{ij})_{(2N+1) \times (2N+1)}$  with  $\begin{cases} \tilde{m}_{ij} = 0 & i \neq j \\ \tilde{m}_{ij} = m_{ij} & i = j \end{cases}$ , and  $\|\cdot\|_F$  is  $F$ -norm.

According to (4), it is easy to know that the mutual coupling of proposed array is smaller than the traditional parallel array [8–11] and larger than unfolded parallel coprime array [20]. But just for the structural feature, the unfolded parallel coprime array cannot be used directly in traditional algorithms such as PM algorithm and estimation of signal parameters via rotational invariance technique (ESPRIT) algorithm [21].

### 3. Description of Improved PM Algorithm

In this section, we introduce the improved PM algorithm based on the proposed array and the algorithm description is based on (2).

Denote the manifold matrix of the whole array as

$$\mathbf{C} = \begin{bmatrix} \mathbf{A}(\boldsymbol{\theta}) \\ \mathbf{B}(\boldsymbol{\theta})\Phi(\boldsymbol{\beta}) \end{bmatrix}. \quad (5)$$

There must be a propagator matrix  $\mathbf{P} \in \mathbb{C}^{K \times (2N+1-K)}$  satisfying [8–10]

$$\mathbf{C}_2 = \mathbf{P}^H \mathbf{C}_1, \quad (6)$$

where  $\mathbf{C}_1$  consists of the first  $K$  rows of matrix  $\mathbf{C}$  and  $\mathbf{C}_2$  consists of the last  $2N+1-K$  rows of matrix  $\mathbf{C}$ .

Denote the covariance matrix  $\mathbf{R} = E[\mathbf{y}(t)\mathbf{y}^H(t)]$ , and it can be partitioned as  $\mathbf{R} = \begin{bmatrix} \mathbf{R}_1 & \mathbf{R}_2 \end{bmatrix}$ , where  $\mathbf{R}_1 \in \mathbb{C}^{(2N+1) \times K}$  and  $\mathbf{R}_2 \in \mathbb{C}^{(2N+1) \times (2N+1-K)}$ .

Then,  $\mathbf{R}$  can be estimated by  $\hat{\mathbf{R}} = (1/T) \sum_{t=1}^T \mathbf{y}(t)\mathbf{y}^H(t)$ , and  $\mathbf{P}$  can be estimated by  $\hat{\mathbf{P}} = (\hat{\mathbf{R}}_1^H \hat{\mathbf{R}}_1)^{-1} \hat{\mathbf{R}}_1^H \hat{\mathbf{R}}_2$  as [8–10], where  $T$  is the number of snapshots.

Construct a block matrix  $\mathbf{P}_o \in \mathbb{C}^{(2N+1) \times K}$ :

$$\mathbf{P}_o = \begin{bmatrix} \mathbf{I}_K \\ \mathbf{P}^H \end{bmatrix} = \begin{bmatrix} \mathbf{P}_z \\ \mathbf{P}_x \end{bmatrix}, \quad (7)$$

where  $\mathbf{P}_z$  is the first  $N+1$  rows of  $\mathbf{P}_o$  and  $\mathbf{P}_x$  is the last  $N$  rows of  $\mathbf{P}_o$ .

According to (7), we can obtain

$$\mathbf{P}_o \mathbf{C}_1 = \mathbf{C}. \quad (8)$$

Combining (7) with (8), we can know

$$\begin{cases} \mathbf{P}_z = \mathbf{A}(\boldsymbol{\theta})\mathbf{C}_1^{-1}, \\ \mathbf{P}_x = \mathbf{B}(\boldsymbol{\theta})\Phi(\boldsymbol{\beta})\mathbf{C}_1^{-1}. \end{cases} \quad (9)$$

Denote  $\mathbf{A}_1(\boldsymbol{\theta})$  as the first  $N$  rows of matrix  $\mathbf{A}(\boldsymbol{\theta})$ ,  $\mathbf{A}_2(\boldsymbol{\theta})$  as the last  $N$  rows of matrix  $\mathbf{A}(\boldsymbol{\theta})$ ,  $\mathbf{B}_1(\boldsymbol{\theta})$  as the first  $N-1$  rows of matrix  $\mathbf{B}(\boldsymbol{\theta})$ , and  $\mathbf{B}_2(\boldsymbol{\theta})$  as the last  $N-1$  rows of matrix  $\mathbf{B}(\boldsymbol{\theta})$ , then we have

$$\begin{cases} \mathbf{P}_1 = \mathbf{A}_1(\boldsymbol{\theta})\mathbf{C}_1^{-1}, \\ \mathbf{P}_2 = \mathbf{A}_2(\boldsymbol{\theta})\mathbf{C}_1^{-1}, \\ \mathbf{P}_3 = \mathbf{B}_1(\boldsymbol{\theta})\Phi(\boldsymbol{\beta})\mathbf{C}_1^{-1}, \\ \mathbf{P}_4 = \mathbf{B}_2(\boldsymbol{\theta})\Phi(\boldsymbol{\beta})\mathbf{C}_1^{-1}, \end{cases} \quad (10)$$

where  $\mathbf{P}_1$  is the first  $N$  rows of  $\mathbf{P}_z$ ,  $\mathbf{P}_2$  is the last  $N$  rows of  $\mathbf{P}_z$ ,  $\mathbf{P}_3$  is the first  $N-1$  rows of  $\mathbf{P}_x$  and  $\mathbf{P}_4$  is the last  $N-1$  rows of  $\mathbf{P}_x$ .

Denote the matrix  $\Psi_1(\boldsymbol{\theta}) = \text{diag}\{e^{-(j2\pi q d \cos \theta_1/\lambda)}, e^{-(j2\pi q d \cos \theta_2/\lambda)}, \dots, e^{-(j2\pi q d \cos \theta_K/\lambda)}\}$ ,  $\Psi_2(\boldsymbol{\theta}) = \text{diag}\{e^{-(j2\pi(q+1)d \cos \theta_1/\lambda)}, e^{-(j2\pi(q+1)d \cos \theta_2/\lambda)}, \dots, e^{-(j2\pi(q+1)d \cos \theta_K/\lambda)}\}$ , and  $\Psi(\boldsymbol{\theta}) = \text{diag}\{e^{-(j2\pi d \cos \theta_1/\lambda)}, e^{-(j2\pi d \cos \theta_2/\lambda)}, \dots, e^{-(j2\pi d \cos \theta_K/\lambda)}\}$ , then we can know

$$\begin{cases} \mathbf{P}_2^+ \mathbf{P}_1 = \mathbf{C}_1 \Psi_1^{-1}(\boldsymbol{\theta}) \mathbf{C}_1^{-1}, \\ \mathbf{P}_3^+ \mathbf{P}_4 = \mathbf{C}_1 \Psi_2(\boldsymbol{\theta}) \mathbf{C}_1^{-1}. \end{cases} \quad (11)$$

According to formula (11), we can get

$$\begin{aligned} \mathbf{P}_2^+ \mathbf{P}_1 \mathbf{P}_3^+ \mathbf{P}_4 &= \mathbf{C}_1 \Psi_1^{-1}(\boldsymbol{\theta}) \mathbf{C}_1^{-1} \mathbf{C}_1 \Psi_2(\boldsymbol{\theta}) \mathbf{C}_1^{-1} \\ &= \mathbf{C}_1 \Psi_1^{-1}(\boldsymbol{\theta}) \Psi_2(\boldsymbol{\theta}) \mathbf{C}_1^{-1} \\ &= \mathbf{C}_1 \Psi(\boldsymbol{\theta}) \mathbf{C}_1^{-1}. \end{aligned} \quad (12)$$

According to formula (12), we have

$$\begin{aligned} \mathbf{P}_z \mathbf{P}_2^+ \mathbf{P}_1 \mathbf{P}_3^+ \mathbf{P}_4 &= \mathbf{A}(\boldsymbol{\theta}) \mathbf{C}_1^{-1} \mathbf{C}_1 \Psi_1^{-1}(\boldsymbol{\theta}) \mathbf{C}_1^{-1} \mathbf{C}_1 \Psi_2(\boldsymbol{\theta}) \mathbf{C}_1^{-1} \\ &= \mathbf{A}(\boldsymbol{\theta}) \Psi(\boldsymbol{\theta}) \mathbf{C}_1^{-1}, \end{aligned} \quad (13)$$

$$\begin{aligned} \mathbf{P}_x \mathbf{P}_2^+ \mathbf{P}_1 \mathbf{P}_3^+ \mathbf{P}_4 &= \mathbf{B}(\boldsymbol{\theta}) \Phi(\boldsymbol{\beta}) \mathbf{C}_1^{-1} \mathbf{C}_1 \Psi_1^{-1}(\boldsymbol{\theta}) \mathbf{C}_1^{-1} \mathbf{C}_1 \Psi_2(\boldsymbol{\theta}) \mathbf{C}_1^{-1} \\ &= \mathbf{B}(\boldsymbol{\theta}) \Phi(\boldsymbol{\beta}) \Psi(\boldsymbol{\theta}) \mathbf{C}_1^{-1}. \end{aligned} \quad (14)$$

Denote two vectors  $\mathbf{e}_{1s} \in C^{q \times 1}$  ( $s = 0, 1, \dots, q-1$ ) and  $\mathbf{e}_{2s} \in C^{(q+1) \times 1}$  ( $s = 0, 1, \dots, q$ ), where the  $(s+1)$ th component of  $\mathbf{e}_{1s}$  or  $\mathbf{e}_{2s}$  is 1, and all the other elements are zeros. Then, we can construct a  $q(N+1) \times (N+1)$  matrix  $\mathbf{E}_{1s} = \mathbf{I}_{N+1} \otimes \mathbf{e}_{1s}$  and a  $N(q+1) \times N$  matrix  $\mathbf{E}_{2s} = \mathbf{I}_N \otimes \mathbf{e}_{2s}$ .

Using formulae (13) and (14), we can obtain two matrices

$$\begin{cases} \mathbf{P}_{newz} = \sum_{s=0}^{q-1} \mathbf{E}_{1s} \mathbf{P}_z (\mathbf{P}_1^+ \mathbf{P}_2 \mathbf{P}_4^+ \mathbf{P}_3)^s = \bar{\mathbf{A}}(\boldsymbol{\theta}) \mathbf{C}_1^{-1}, \\ \mathbf{P}_{newx} = \sum_{s=0}^q \mathbf{E}_{2s} \mathbf{P}_x (\mathbf{P}_1^+ \mathbf{P}_2 \mathbf{P}_4^+ \mathbf{P}_3)^s = \bar{\mathbf{B}}(\boldsymbol{\theta}) \Phi(\boldsymbol{\beta}) \mathbf{C}_1^{-1}, \end{cases} \quad (15)$$

where  $\bar{\mathbf{A}}(\boldsymbol{\theta}) = [\bar{\mathbf{a}}(\theta_1), \dots, \bar{\mathbf{a}}(\theta_K)] \in C^{q(N+1) \times K}$ ,  $\bar{\mathbf{a}}(\theta_k) = [1, e^{-(j2\pi d \cos \theta_k/\lambda)}, \dots, e^{-(j2\pi(q(N+1)-1)d \cos \theta_k/\lambda)}]^T \in C^{q(N+1) \times 1}$ ,  $\bar{\mathbf{B}}(\boldsymbol{\theta}) = [\bar{\mathbf{b}}(\theta_1), \dots, \bar{\mathbf{b}}(\theta_K)] \in C^{N(q+1) \times K}$  and  $\bar{\mathbf{b}}(\theta_k) = [1, e^{-(j2\pi d \cos \theta_k/\lambda)}, \dots, e^{-(j2\pi[(q+1)N-1]d \cos \theta_k/\lambda)}]^T \in C^{N(q+1) \times 1}$ .

Denote a matrix

$$\mathbf{P}'_{newx} = \mathbf{P}_{newx} (1: q(N+1), :), \quad (16)$$

where  $\mathbf{P}_{newx} (1: q(N+1), :)$  consists of the first  $q(N+1)$  rows of  $\mathbf{P}_{newx}$ .

Combining (15) with (16), we have

$$\mathbf{P}_{newz}^+ \mathbf{P}'_{newx} = \mathbf{C}_1 \Phi(\boldsymbol{\beta}) \mathbf{C}_1^{-1}. \quad (17)$$

Performing EVD of  $\mathbf{P}_2^+ \mathbf{P}_1 \mathbf{P}_3^+ \mathbf{P}_4$  and  $\mathbf{P}_{newz}^+ \mathbf{P}'_{newx}$  can obtain the eigenvalues of the two matrices. Let the eigenvalues of  $\mathbf{P}_2^+ \mathbf{P}_1 \mathbf{P}_3^+ \mathbf{P}_4$  and  $\mathbf{P}_{newz}^+ \mathbf{P}'_{newx}$  be  $\lambda_1, \lambda_2, \dots, \lambda_K$  and  $\gamma_1, \gamma_2, \dots, \gamma_K$ , then we can get the estimation of  $\theta_k, \beta_k$  as

$$\hat{\theta}_k = \arccos\left(\frac{\lambda \text{angle}(\lambda_k)}{2\pi d}\right), \quad (18)$$

$$\hat{\beta}_k = \arccos\left(\frac{\lambda \text{angle}(\gamma_k)}{2\pi d}\right). \quad (19)$$

Using the pairing method [8], we can get the matched 2D DOA estimations.

According to (14), we can know that the row number of  $\mathbf{P}_{newz}$  and  $\mathbf{P}'_{newx}$  are larger than  $\mathbf{P}_z$  and  $\mathbf{P}_x$ . Hence, the construction of  $\mathbf{P}_{newz}$  and  $\mathbf{P}'_{newx}$  also can see the process of adding the virtual sensors of array. For traditional non-uniform array, spatial smoothing algorithm [14] is the widely used method to obtain extended covariance matrix. And DOA is estimated by dealing with the extended covariance matrix in some existing algorithm. Certainly, this process is different from the proposed algorithm.

## 4. Complexity Analysis

In this section, the complexity of proposed algorithm is compared with PM [8–10]. Suppose that the two-parallel array consisting of an  $(L+1)$ -element linear array and an  $L$ -element linear array for the proposed algorithm and PM [8, 9]. Consider an  $(L+1)$ -element linear array and two  $L/2$ -element linear arrays for PM [10]. Assume that  $L \ll T$ , so we only consider the complexity of main step for four PM algorithms. Both the complexity of PM [9] and proposed PM are  $O\{(2L+1)^2 T\}$ . The complexity of PM [8] and PM [10] is  $O\{(3L)^2 T\}$  and  $O\{L(L+1)T\}$ , respectively. Figure 4 lists the comparison of complexity versus snapshots with  $L=10$ . Figure 5 lists the comparison of complexity versus the number of sensors with  $T=500$ .

## 5. Simulation

In this section, we perform several groups of simulation experiments to confirm the outstanding effectiveness of proposed algorithm in reducing coupling and improving estimation precision. In [9], authors have proved that the accuracy of PM [8] is lower than PM [9], and complexity of PM [8] is higher than PM [9]. Hence, we only compare the proposed algorithm with PM [9, 10]. In the first three experiments, assume that a 21-element two-parallel array is used for the PM [9] and the proposed PM algorithm, and a 21-element three-parallel array are used for PM [10]. Suppose that the elevation and azimuth angles of three signals are  $[\theta_1, \theta_2, \theta_3] = [50^\circ, 60^\circ, 70^\circ]$  and  $[\beta_1, \beta_2, \beta_3] = [40^\circ, 50^\circ, 60^\circ]$ . Denote  $\hat{\theta}_{kj}$  and  $\hat{\beta}_{kj}$  as the estimations of  $\theta_k$  and  $\beta_k$  in the  $j$ th experiment, respectively. For the sake of fair comparison, only accurate pairing estimation

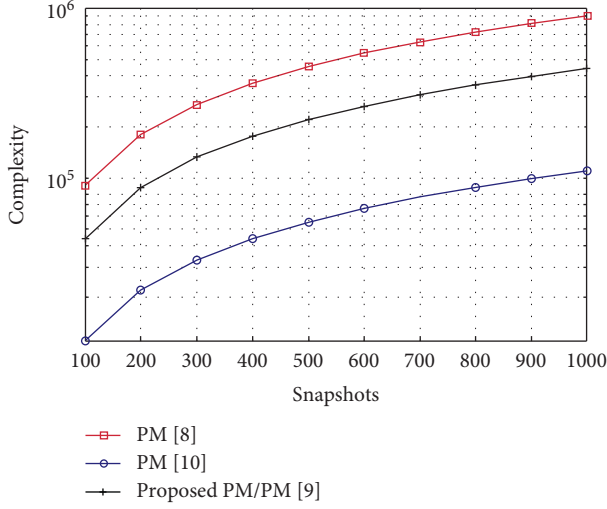


FIGURE 4: Complexity versus snapshots.

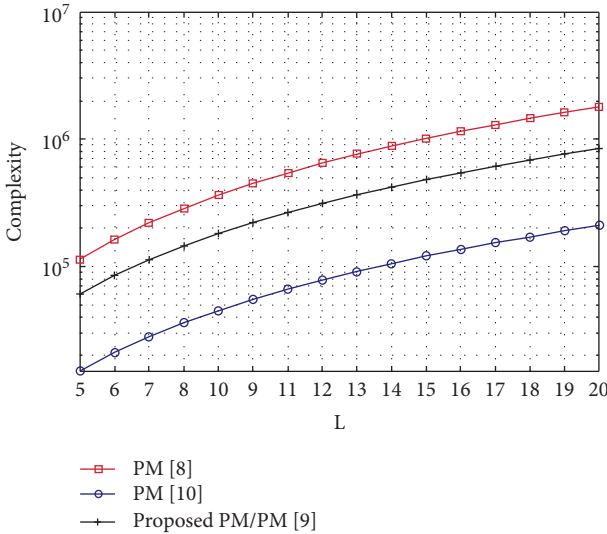


FIGURE 5: Complexity versus the number of sensors.

results are given in the experiment. We denote the root mean square error (RMSE) of 2D DOA estimation as

$$\text{RMSE} = \sqrt{\frac{1}{KJ} \sum_{j=1}^J \sum_{k=1}^K \left\{ (\hat{\theta}_{kj} - \theta_k)^2 + (\hat{\beta}_{kj} - \beta_k)^2 \right\}}, \quad (20)$$

where  $J=1000$  is the number of repeated experiments.

Firstly, we compare the estimation precision of three PM algorithms in the absence of mutual coupling. Figure 6 lists the comparison result of RMSE for three PM algorithms and CRLB [9] versus SNR with 500 snapshots. Figure 7 lists the comparison result of RMSE for three PM algorithms and CRLB versus the number of snapshots with 5 dB SNR. According to the results shown in the two figures, we can see that the estimation precision of proposed PM and PM [9] is far higher than the PM [10], and the estimation precision of proposed PM is slightly higher than PM [9] under high SNR.

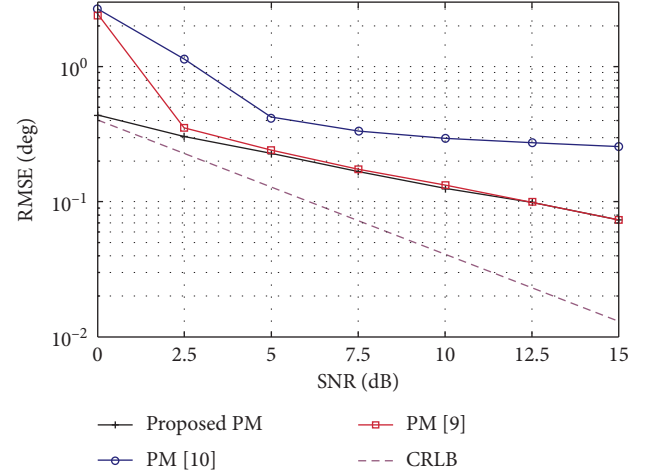


FIGURE 6: RMSE of three PM algorithms versus SNR.

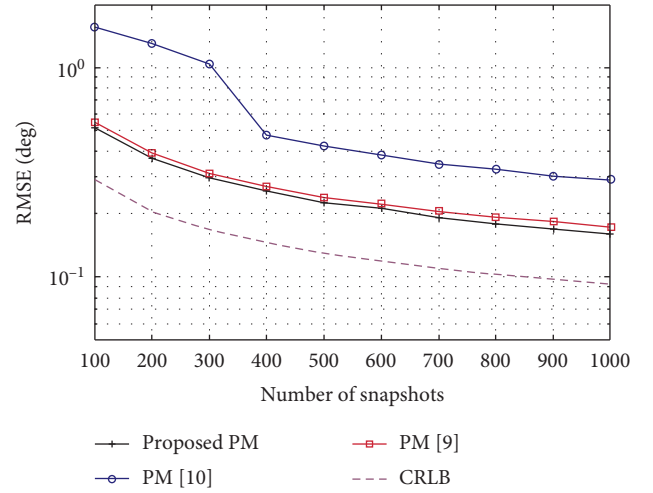


FIGURE 7: RMSE of three PM algorithms versus the number of snapshots.

But the proposed PM algorithm shows significant advantage when the SNR is lower, which can be seen from Figure 6.

Secondly, we compare the performance of the proposed method for different  $q$  in the absence of mutual coupling. Figure 8 lists the comparison result of RMSE versus SNR with 500 snapshots. Figure 9 lists the comparison result of RMSE for different  $q$  versus the number of snapshots with 5 dB SNR. The results in the two figures indicate that the performance of the proposed method can be improved slightly as the growth of  $q$ . Combining the results of Figures 8 and 9, we can know that the estimation precision can be improved as the extension of aperture under the same number of sensors. Since the row number of  $\mathbf{P}_{newz}$ ,  $\mathbf{P}_{newx}'$  is larger than  $\mathbf{P}_z$ ,  $\mathbf{P}_x$ , it is reasonable to find that the proposed algorithm can improve the estimation precision.

Thirdly, we compare the estimation performance of the PM algorithm [9] and proposed algorithm in the appearance of mutual coupling. We only suppose that the mutual coupling effect only exist between two sensors with the interval no further than  $d$ . Let  $c_1 = 0.1e^{j\pi}$  be the mutual



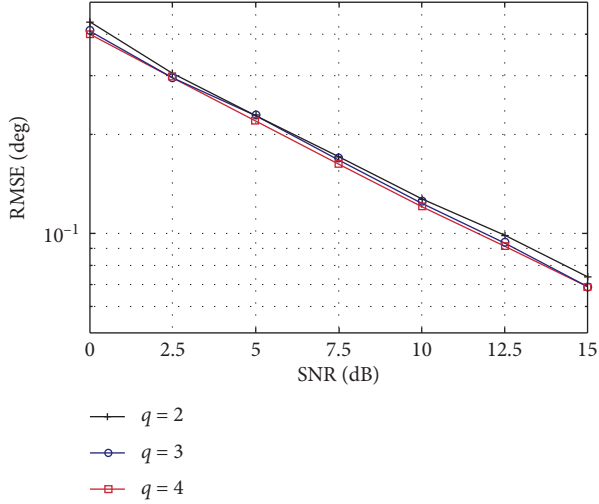


FIGURE 8: RMSE of the proposed algorithm with different  $q$  versus SNR.

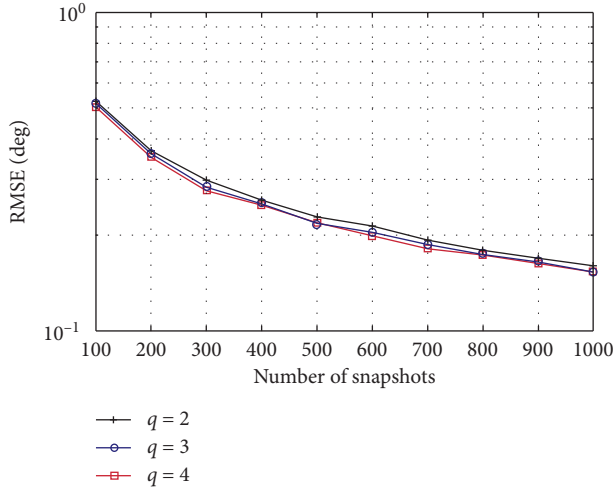


FIGURE 9: RMSE of the proposed algorithm with different  $q$  versus snapshots.

coupling coefficient between two sensors with interval  $d$ , and  $c_0 = 1$  be the self-couple coefficient. Fix SNR at 15 dB and the number of snapshots at 500. Figures 10 and 11 display 100 estimation results of proposed algorithm and PM algorithm [9], respectively. It is clear to see that the estimation error of proposed PM is smaller than the PM [9]. The results also can prove the effectiveness of the proposed array in reducing mutual coupling.

At last, we test the estimation performance of proposed algorithm for more signals with small interval.

Assume that the proposed array consists of a 25-element array and a 26-element array. Suppose that the elevation and azimuth angles of fifteen signals are  $[\theta_1, \theta_2, \theta_3, \theta_4, \theta_5, \theta_6, \theta_7, \theta_8, \theta_9, \theta_{10}, \theta_{11}, \theta_{12}, \theta_{13}, \theta_{14}, \theta_{15}] = [10^\circ, 15^\circ, 20^\circ, 25^\circ, 30^\circ, 35^\circ, 40^\circ, 45^\circ, 50^\circ, 55^\circ, 60^\circ, 65^\circ, 70^\circ, 75^\circ, 80^\circ]$  and  $[\beta_1, \beta_2, \beta_3, \beta_4, \beta_5, \beta_6, \beta_7, \beta_8, \beta_9, \beta_{10}, \beta_{11}, \beta_{12}, \beta_{13}, \beta_{14}, \beta_{15}] = [5^\circ, 10^\circ, 45^\circ, 25^\circ, 20^\circ, 30^\circ, 35^\circ, 40^\circ, 15^\circ, 75^\circ, 55^\circ, 50^\circ, 65^\circ, 70^\circ, 60^\circ]$ . Fix SNR at 20dB and the number of snapshots at 1000. Figure 12 displays 100

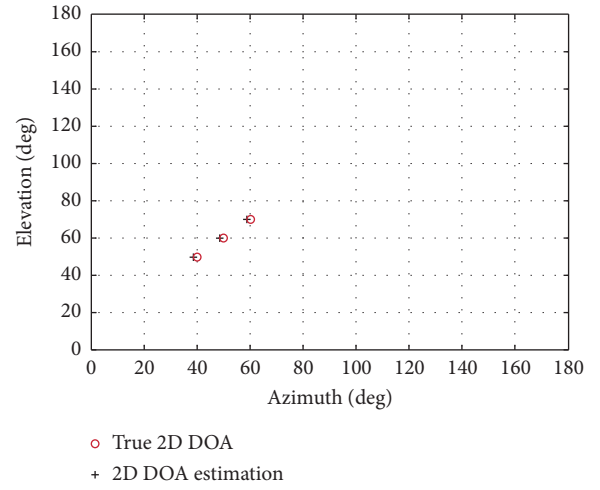


FIGURE 10: DOA estimation results of the proposed method with  $c_1 = 0.1e^{j\pi}$ .

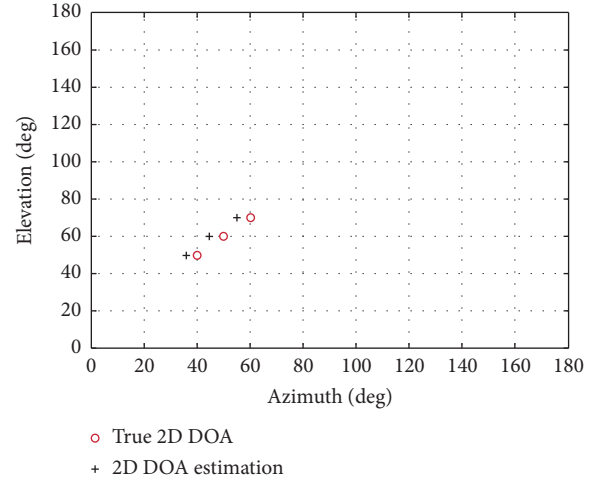


FIGURE 11: DOA estimation results of PM [9] with  $c_1 = 0.1e^{j\pi}$ .

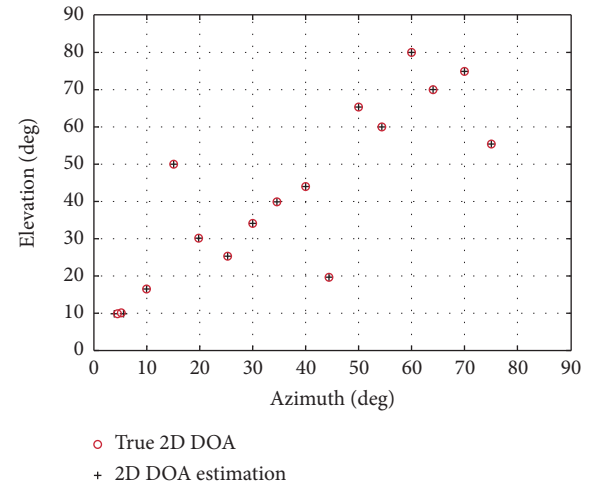


FIGURE 12: DOA estimation results of the proposed method for small interval signals.

estimation results of the proposed algorithm. The result in this figure can show that the proposed algorithm can distinguish many signals with small interval, but it needs a large number of sensors.

## 6. Conclusion

In this paper, we have proposed an improved 2D PM algorithm with a two-parallel array consisting of two uniform linear arrays, the spacing of which is larger than half a wavelength of the incident signal. The proposed algorithm has higher estimation precision than many existed 2D PM algorithms. Due to the large-spacing of proposed array, mutual coupling can be reduced. The proposed algorithm has better performance than the traditional algorithm under mutual coupling. But because no decoupling algorithm is used for the proposed algorithm, the error of the DOA estimate is still significant under mutual coupling. In future research, according to the proposed two-parallel array, we will work for presenting the decoupling algorithm like [22, 23].

## Data Availability

In this paper, we use simulation to test the performance of proposed algorithm. Hence, all data are generated by simulation. The simulation data used to support the findings of this study are available from the corresponding author upon request.

## Conflicts of Interest

The authors declare that there are no conflicts of interest regarding the publication of this paper.

## Acknowledgments

This work was supported by the National Natural Science Foundation of China (51877015 and U1831117), the Cooperation Agreement Foundation by the Department of Science and Technology of Guizhou Province of China (LH [2017]7320 and LH[2017]7321), the Innovation Group Major Research Program Funded by Guizhou Provincial Education Department (KY[2016]051), the Foundation of Top-notch Talents by Education Department of Guizhou Province of China (KY[2018]075), and PhD Research Startup Foundation of Tongren University (trxyDH1710).

## References

- [1] J. Su, Z. Sheng, V. C. M. Leung, and Y. Chen, "Energy efficient tag identification algorithms for RFID: survey, motivation and new design," *IEEE Wireless Communications*, vol. 26, no. 3, pp. 118–124, 2019.
- [2] J. Shi, G. Hu, X. Zhang, F. Sun, W. Zheng, and Y. Xiao, "Generalized co-prime MIMO radar for DOA estimation with enhanced degrees of freedom," *IEEE Sensors Journal*, vol. 18, no. 3, pp. 1203–1212, 2018.
- [3] S. Liu, L. Yang, D. Li, and H. Cao, "Subspace extension algorithm for 2D DOA estimation with L-shaped sparse array," *Multidimensional Systems and Signal Processing*, vol. 28, no. 1, pp. 315–327, 2017.
- [4] N. Tayem and H. M. Kwon, "L-shape 2-dimensional arrival angle estimation with propagator method," *IEEE Transactions on Antennas and Propagation*, vol. 53, no. 5, pp. 1662–1630, 2005.
- [5] Q. Y. Yin, L. H. Zou, and R. W. Newcomb, "A high resolution approach to 2-D signal parameter estimation-DOA matrix method," *Journal of China Institute of Communications*, vol. 12, no. 4, pp. 1–7, 1991.
- [6] T. Xia, Y. Zheng, Q. Wan, and X. Wang, "Decoupled estimation of 2-D angles of arrival using two parallel uniform linear arrays," *IEEE Transactions on Antennas and Propagation*, vol. 55, no. 9, pp. 2627–2632, 2007.
- [7] Y. Zhang, X. Xu, Y. A. Sheikh, and Z. Ye, "A rank-reduction based 2-D DOA estimation algorithm for three parallel uniform linear arrays," *Signal Processing*, vol. 120, pp. 305–310, 2016.
- [8] Y. Wu, G. Liao, and H. C. So, "A fast algorithm for 2-D direction-of-arrival estimation," *Signal Processing*, vol. 83, no. 8, pp. 1827–1831, 2003.
- [9] J. Li, X. Zhang, and H. Chen, "Improved two-dimensional DOA estimation algorithm for two-parallel uniform linear arrays using propagator method," *Signal Processing*, vol. 92, no. 12, pp. 3032–3038, 2012.
- [10] L. Yang, S. Liu, D. Li, H. L. Cao, and Q. P. Jiang, "Fast 2D DOA estimation algorithm by an array manifold matching method with parallel linear arrays," *Sensors*, vol. 16, no. 3, p. 274, 2016.
- [11] N. Tayem, K. Majeed, and A. A. Hussain, "Propagator method using PARAFAC model for two dimensional source localization," *Radioengineering*, vol. 27, no. 3, pp. 770–775, 2018.
- [12] S. Marcos, A. Marsal, and M. Benidir, "The propagator method for source bearing estimation," *Signal Processing*, vol. 42, no. 2, pp. 121–138, 1995.
- [13] S. Liu, L. Yang, J. H. Huang, and Q. P. Jiang, "Generalization propagator method for DOA estimation," *Progress in Electromagnetics Research M*, vol. 37, pp. 119–125, 2014.
- [14] M. Yang, A. M. Haimovich, X. Yuan, L. Sun, and B. Chen, "A unified array geometry composed of multiple identical sub-arrays with hole-free difference coarrays for underdetermined DOA estimation," *IEEE Access*, vol. 6, pp. 14238–14254, 2018.
- [15] C.-L. Liu and P. P. Vaidyanathan, "Super nested arrays: linear sparse arrays with reduced mutual coupling—part I: fundamentals," *IEEE Transactions on Signal Processing*, vol. 64, no. 15, pp. 3997–4012, 2016.
- [16] C.-L. Liu and P. P. Vaidyanathan, "Super nested arrays: linear sparse arrays with reduced mutual coupling—part II: high-order extensions," *IEEE Transactions on Signal Processing*, vol. 64, no. 16, pp. 4203–4217, 2016.
- [17] J. Liu, Y. Zhang, Y. Lu, S. Ren, and S. Cao, "Augmented nested arrays with enhanced DOF and reduced mutual coupling," *IEEE Transactions on Signal Processing*, vol. 65, no. 21, pp. 5549–5563, 2017.
- [18] W. Zheng, X. Zhang, P. Gong, and H. Zhai, "DOA estimation for co-prime linear arrays: an ambiguity-free method involving full DOFs," *IEEE Communications Letters*, vol. 22, no. 3, pp. 562–565, 2018.
- [19] P. Pal and P. P. Vaidyanathan, "Coprime sampling and the MUSIC algorithm," in *Proceedings of the Digital Signal Processing Workshop and IEEE Signal Processing Education Workshop (DSP/SPE)*, pp. 289–294, Sedona, AZ, USA, January 2011.
- [20] J. Li, Y. Li, and X. Zhang, "Two-dimensional off-grid DOA estimation using unfolded parallel coprime array," *IEEE Communications Letters*, vol. 22, no. 12, pp. 2495–2498, 2018.

- [21] R. Roy and T. Kailath, "ESPRIT-estimation of signal parameters via rotational invariance techniques," *IEEE Transactions on Acoustics, Speech, and Signal Processing*, vol. 37, no. 7, pp. 984–995, 1989.
- [22] Z. Ye and C. Liu, "On the resiliency of music direction finding against antenna sensor coupling," *IEEE Transactions on Antennas and Propagation*, vol. 56, no. 2, pp. 371–380, 2008.
- [23] S. Liu, J. Zhao, and Z. Xiao, "DOA estimation with sparse array under unknown mutual coupling," *Progress in Electromagnetics Research Letters*, vol. 70, pp. 147–153, 2017.